IARJSET ISSN (O) 2393-8021, ISSN (P) 2394-1588

International Advanced Research Journal in Science, Engineering and Technology

Impact Factor 8.311 ⁜ Peer-reviewed & Refereed journal ⁜ Vol. 13, Issue 5, May 2026

DOI: 10.17148/IARJSET.2026.13569

# Mechanical Characterization of an *Eucheuma cottonii* White Seaweed-Based Bioplastic Film: Effect of seafood Protein and Sorbitol Plasticizer on Tensile Properties

**Nicolas Meuley[1,2], Tjokorda Gde Tirta Nindhia[2]*, Ade Saepullah[3], Agri Kala Yosua[3]**

Polytech Lyon, Department of Mechanical Engineering, Université Claude Bernard Lyon 1, France[1]

Study Program of Mechanical Engineering, Faculty of Engineering, Udayana University, Bali, Indonesia[2]

Study Program of Master in Mechanical Engineering, Faculty of Engineering, Udayana University, Bali, Indonesia[3]

*Correspondent Author: tirta.nindhia@me.unudac.id/nindhia@yahoo.com

**Abstract‡** This work reports the preliminary mechanical characterization of a bioplastic film prepared from white Eucheuma cottonii seaweed, using sorbitol as a plasticizer and a small fraction of seafood protein as a reinforcing additive. The film was cast from an acid-extracted seaweed slurry and dried under ambient ventilated conditions. Tensile tests were carried out on four specimens whose geometry was inspired by the ASTM D638 Type V standard, using a manual screw-driven apparatus instrumented with an analog force gauge (capacity 10 N, resolution 0.05 N) and a digital dial indicator (resolution 0.01 mm). After removing the zero-load take-up artifacts observed at the beginning of each test, the mean ultimate tensile strength was found to be 2.67(76) MPa, the mean strain at break 1.01 0.17, and the mean Young's modulus, determined from a linear regression on the initial elastic region, was 1.97(62) MPa. Optical microscopy revealed millimetre-scale residual porosities and an inhomogeneous through- thickness distribution of unfiltered fibers, which are identified as the primary mechanical weak points of the current formulation. Comparison with the existing literature on Eucheuma cottonii and Gracilaria films suggests that the unusually low stiffness and high apparent strain at break observed here reflect both the high plasticizer- to-polymer ratio of the formulation and the limitations of the testing setup, which are discussed in detail.

**Keywords:** bioplastic; Eucheuma cottonii; alginate; sorbitol; seafood protein; tensile testing.

## 1. INTRODUCTION

The rapid accumulation of petroleum-based plastic waste in marine environments has accelerated the search for biodegradable alternatives derived from renewable resources. Seaweed-based bioplastics are particularly attractive in tropical archipelagic countries such as Indonesia, where large-scale cultivation of red algae *Eucheuma cottonii* already supports an established carrageenan industry. The polysaccharides extracted from *Eucheuma cottonii* (predominantly $\kappa$- carrageenan, and, depending on extraction conditions, fractions of alginate-like macromolecules) are known to form self-standing films upon casting and drying [2, 4].

Two persistent issues limit the practical use of such films. First, their mechanical performance is highly sensitive to the type and concentration of plasticizer, with glycerol, sorbitol and polyethylene glycol all re- ported to dramatically increase the strain at break at the expense of strength and stiffness [6, 7]. Second, the films are typically brittle and porous when no reinforcement is added, motivating the inclusion of protein or cellulose fillers to improve homogeneity and ductility [5, 8].

Most published works on *Eucheuma cottonii* films use the brown or green commercial grade of the algae. White-grade *Eucheuma cottonii*, obtained after sun-bleaching of the harvested algae, is more readily available in retail markets in Bali but has received considerably less attention in the bioplastic literature. The present study reports the fabrication and tensile char- acterization of a film prepared from white *Eucheuma cottonii*, plasticized with sorbitol and reinforced with a small fraction of seafood protein. The mechanical results are interpreted in the light of optical microscopy observations of the fracture region, and the limitations of the simplified testing apparatus used here are explicitly discussed.

IARJSET ISSN (O) 2393-8021, ISSN (P) 2394-1588

International Advanced Research Journal in Science, Engineering and Technology

Impact Factor 8.311 ⁜ Peer-reviewed & Refereed journal ⁜ Vol. 13, Issue 5, May 2026

DOI: 10.17148/IARJSET.2026.13569

## 2. MATERIALS AND METHODS

### 2.1. *Raw Materials*

Dried white *Eucheuma cottonii* seaweed was purchased in Bali, Indonesia. Distilled water was used through- out. White vinegar (cuka putih, ≈ 4 % to 5 % acetic acid, food grade) was used as the extraction acid. Sorbitol (food grade) was used as the plasticizer, and a commercial powdered marine (seafood) protein concentrate was added as a reinforcing additive. Sodium chloride (NaCl, analytical grade) was used to adjust the ionic strength of the solution.

### 2.2. *Film Preparation*

The bioplastic films were prepared according to the following procedure:

1. *Rehydration.* 15 g of dried white algae were cleaned and soaked in distilled water (mass ratio approximately 1:3) for 1 h until the algae became soft and swollen, then drained.

2. *Acid solution.* A 1 % (v/v) acetic acid solution was prepared by diluting the commercial vinegar in distilled water (final volume 200 mL).

3. *Mixing.* The rehydrated algae and the acid solution were mixed in a kitchen blender for approximately 5 min until a homogeneous slurry was obtained.

4. *Hot extraction.* The slurry was transferred to a stainless-steel pan and heated to 85 ◦C to 90 ◦C under constant stirring for 10 min, allowing the acid to disrupt the cell walls and release the polysaccharides.

5. *Filtration.* The hot mixture was filtered through a fine cloth (*kain saring*), pressed to extract the maximum amount of liquid, and the solid residue was discarded.

6. *Plasticizer addition.* The filtrate was returned to the pan, the temperature reduced to 45 ◦C to 50 ◦C, and 7 mL of sorbitol were added under continuous stirring for 5 min.

7. *Protein addition.* 5 g of marine protein were dis- solved in approximately 30 mL of warm distilled water, added to the pan, and stirred for an additional 5 min.

8. *Ionic adjustment.* 0.5 g of NaCl were added to stabilize the colloidal phase.

9. *Casting.* The warm mixture was poured onto a clean flat glass plate, with 4 mm thick spacers placed along the edges as thickness guides. A spat- ula was used to level the surface against the guides.

10. *Drying.* The plate was placed in an airconditioned room maintained at 23 ◦C, with a low- speed fan directed at the casting surface. The film was turned on day 2 to allow uniform drying on both sides. The total drying time was 4 d to 5 d, and the film was considered ready when it no longer felt tacky and its edges detached spontaneously from the plate.

The final film thickness after drying was reduced to approximately 0.2 mm due to evaporation of the aque- ous phase. Specimens were cut manually from the cen- tral region of the dried film with a scalpel and a metallic template.

### 2.3. *Specimen Geometry*

The specimen geometry was inspired by the ASTM D638 Type V dogbone [1]. The nominal dimensions used in this study were: gauge length $L_0 = 9$ mm, narrow-section width $w = 3$ mm, and thickness $t = 0.2$ mm, giving an initial cross-sectional area $A_0 = w\ t = 0.6$ mm$^2$. The gauge length is slightly larger than the 7.62 mm prescribed by ASTM D638 Type V; the difference is acknowledged here and is taken into account in the discussion of the results. A photograph of the dried film prior to cutting is shown in Fig.1.

IARJSET ISSN (O) 2393-8021, ISSN (P) 2394-1588

International Advanced Research Journal in Science, Engineering and Technology

Impact Factor 8.311 ⁜ Peer-reviewed & Refereed journal ⁜ Vol. 13, Issue 5, May 2026

DOI: 10.17148/IARJSET.2026.13569

Figure 1: Dried white *Eucheuma cottonii* bioplastic film on the glass casting plate, prior to being cut into specimens. The film is approximately 0.2 mm thick. Dogbone specimens with the geometry described in Section 2.3 were hand-cut from the central region of the film with a scalpel and a metallic template.

### 2.4. *Tensile Testing Apparatus*

Tensile tests were performed using a manual screw- driven apparatus (Fig. 2) instrumented with an analog force gauge (model NK-10, nominal capacity 10 N, resolution 0.05 N) and a digital dial indicator (resolution 0.01 mm) used to record the crosshead displacement. The load was applied manually through a screw drive in small increments, and at each increment the force reading and the displacement reading were recorded simultaneously. This setup does not impose a constant strain rate and therefore does not strictly comply with the loading conditions of ASTM D638; it is consistent with the simplified tensile characterization methods commonly employed for thin biopolymer films in low-resource laboratory contexts. The implications of this choice are discussed in Section 4.


Figure 2: Manual tensile testing apparatus used in this study. The specimen is gripped between the lower fixed clamp and the upper crosshead linked to the analog force gauge (model NK-10, 10 N). Crosshead displacement is recorded by the digital dial indicator on the left.

IARJSET ISSN (O) 2393-8021, ISSN (P) 2394-1588

International Advanced Research Journal in Science, Engineering and Technology

Impact Factor 8.311 ⁜ Peer-reviewed & Refereed journal ⁜ Vol. 13, Issue 5, May 2026

DOI: 10.17148/IARJSET.2026.13569

The engineering stress $\sigma$ and engineering strain $\varepsilon$ were computed from the measured force $P$ and elongation $\Delta L$ as:

$$\sigma = \frac{P}{A_0}, \qquad \varepsilon = \frac{\Delta L}{L_0}. \tag{1}$$

Tests were conducted at room temperature (23 °C) and ambient relative humidity. Four specimens (S1– S4) were tested.

### 2.5. *Data Processing*

For each specimen, the raw stress–strain data con- tained a series of initial points at $\sigma = 0$ but with non- zero displacement, attributed to the take-up of slack in the grips and to the manual mise-en-charge of the apparatus. These take-up points were systematically removed (between 12 and 30 leading points per spec- imen) and the strain axis was shifted so that $\varepsilon = 0$ corresponds to the first non-zero force reading. Fig- ure 3 illustrates this procedure for specimen S2.

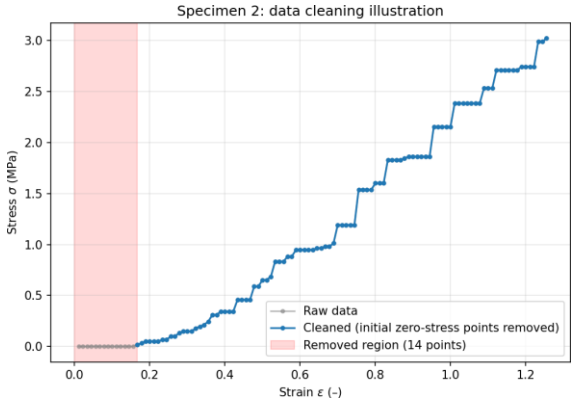


Figure 3: Illustration of the data-cleaning procedure on specimen S2. The initial points (red region) are recorded at $\sigma = 0$ and correspond to the take-up of slack in the apparatus; they are removed and the strain axis is shifted so that $\varepsilon = 0$ coincides with the first non- zero force reading.

The Young's modulus $E$ was determined for each specimen as the slope of a least-squares linear regres- sion performed on the lowest 25% of the strain range, which approximately corresponds to the initial pseudo- linear elastic region observed in the cleaned curves (Fig. 4). The ultimate tensile strength (UTS) was taken as the maximum stress recorded, and the strain at break $\varepsilon_{max}$ as the corresponding strain.

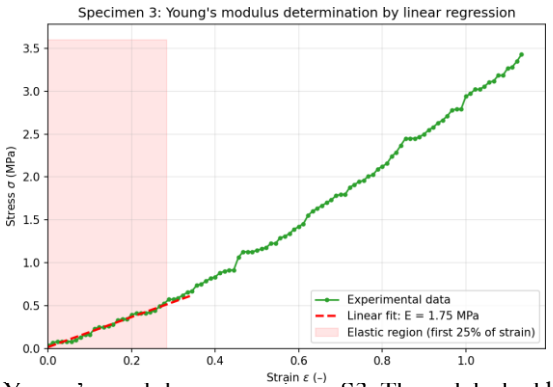


Figure 4: Determination of the Young's modulus on specimen S3. The red dashed line is a linear regression performed on the first 25% of the strain range (shaded region), yielding $E = 1.75$ MPa for this specimen.

### 2.6. *Optical Microscopy*

After fracture, the specimens were observed with a digital optical microscope to inspect the fracture surface, the bulk porosity, and the through-thickness homogeneity. A calibration image of a steel rule with 1 mm graduation was acquired with identical optical settings (Fig. 5) and used to convert the pixel coordinates of the micrographs into physical lengths.

IARJSET ISSN (O) 2393-8021, ISSN (P) 2394-1588

International Advanced Research Journal in Science, Engineering and Technology

Impact Factor 8.311 ⁜ Peer-reviewed & Refereed journal ⁜ Vol. 13, Issue 5, May 2026

DOI: 10.17148/IARJSET.2026.13569

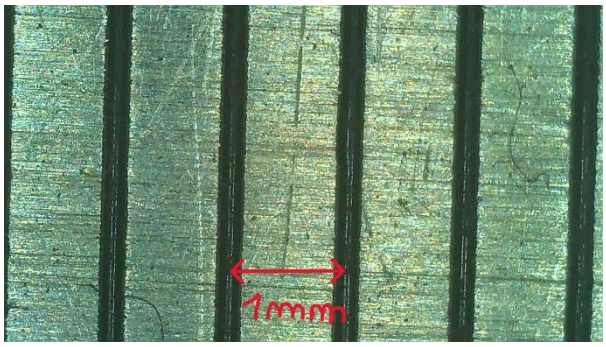


Figure 5: Calibration image: 1 mm graduation of a steel rule, photographed with the same microscope set- tings as the bioplastic micrographs.

## 3. RESULTS

### 3.1. *Tensile Behavior*

The cleaned stress–strain curves of the four specimens are presented in Fig. 6. All four specimens exhibit a qualitatively similar behavior: a short initial pseudo- linear region (up to $\varepsilon \approx 0.1$–$0.2$), followed by an ex- tended non-linear regime in which the stress increases progressively up to the ultimate tensile strength, with- out a clearly defined yield point. No pronounced strain- softening was observed before failure.

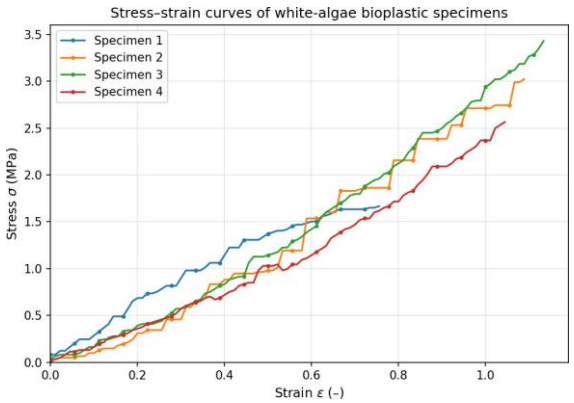


Figure 6: Cleaned stress–strain curves of the four white *Eucheuma cottonii* bioplastic specimens (S1–S4).

Specimen S1 deviates noticeably from the other three: it reaches a lower UTS (1.67 MPa) and breaks at a smaller strain ($\varepsilon_{max} = 0.76$), while specimens S2–S4 cluster between 2.56 and 3.43 MPa and break at strains in the range 1.04 to 1.13. The slope of the initial re- gion is also visibly higher for S1, leading to a Young's modulus (2.89 MPa) that is approximately 60 % higher than the average of the other three specimens.

Table 1: Tensile properties measured on the four specimens.

| Specimen | $\sigma$max (MPa) | $\varepsilon$max | $E$ (MPa) |
|---|---|---|---|
| S1 | 1.67 | 0.76 | 2.89 |
| S2 | 3.02 | 1.09 | 1.50 |
| S3 | 3.43 | 1.13 | 1.75 |
| S4 | 2.56 | 1.04 | 1.74 |
| Mean | **2.67** | **1.01** | **1.97** |
| SD | 0.76 | 0.17 | 0.62 |
| CV (%) | 28 | 17 | 32 |

The individual values and the corresponding statistics (mean, standard deviation, coefficient of variation)are summarized in Table 1. The coefficients of variation are large (17 % to 32 %), which is consistent with the limited number of specimens and with the manual nature of both the specimen preparation and the testing.

Figure 7 provides a graphical comparison of the three mechanical metrics per specimen and highlights the outlying character of specimen S1.

IARJSET ISSN (O) 2393-8021, ISSN (P) 2394-1588

International Advanced Research Journal in Science, Engineering and Technology

Impact Factor 8.311 ⁜ Peer-reviewed & Refereed journal ⁜ Vol. 13, Issue 5, May 2026

DOI: 10.17148/IARJSET.2026.13569

### 3.2. *Optical Microscopy of the Fracture Region*

Figure 8 shows the fracture region of a representative specimen. The fracture path is irregular and propagates through several pre-existing porosities, the principal ones being highlighted in Fig. 9. The largest defect is approximately 0.4 mm long, i.e. of the order of 15 % of the specimen width. Smaller voids, typically 0.05 mm to 0.15 mm in diameter, are distributed throughout the bulk of the specimen and are interpreted as residual gas bubbles trapped during the casting step.

## 4. DISCUSSION

### 4.1. *Comparison with the Literature*

The mean ultimate tensile strength obtained in this study (2.67 MPa) is of the same order of magnitude as values reported by Consebit *et al.* [4] for *Eucheuma cottonii* -based films plasticized with glycerol, and by Saepullah *et al.* [3] for *Gracilaria*-based films (2 MPa to 8 MPa depending on processing conditions). The strain at break measured here ($\varepsilon_{max}$ 1.0, i.e. 100 %), how- ever, is markedly higher than the values typically re- ported in the literature for similar seaweed-based films, which lie in the range 0.05 to 0.40[6, 7, 8]. Two contributions are likely to explain this discrepancy.

First, the formulation used in this study contains a substantial fraction of sorbitol (7 mL for an initial seaweed mass of 15 g). Sorbitol is known to plasticize polysaccharide films very efficiently, reducing the stiffness and the strength while greatly increasing the strain at break [6]. The combination of a low Young's modulus (1.97 MPa, more than one order of magnitude lower than typical values reported for carrageenan films plasticized with glycerol at lower mass ratios) and a high strain at break is qualitatively consistent with an over-plasticized formulation.

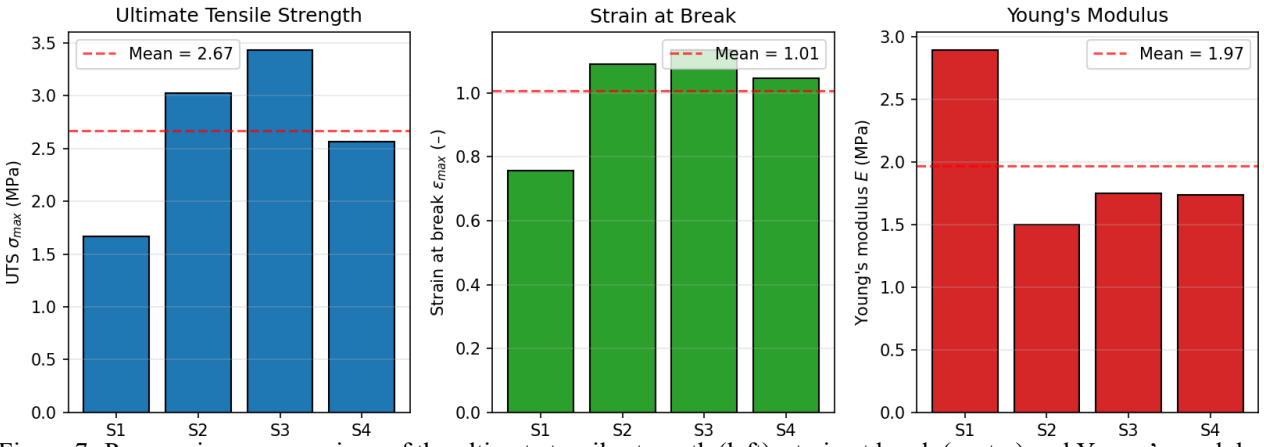


Figure 7: Per-specimen comparison of the ultimate tensile strength (left), strain at break (centre) and Young's modulus (right). The red dashed line indicates the mean over the four specimens.

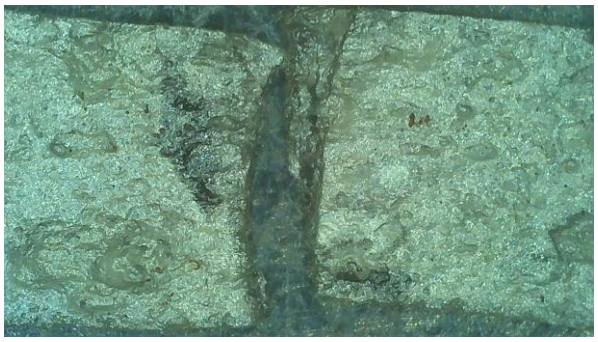

Figure 8: Optical micrograph of the fracture region of a representative specimen. The fracture line is visible at the centre of the field of view; pre-existing porosities are visible on both sides of the fracture path. Field of view approximately 4 mm wide (see calibration in Fig. 5).

Second, the measured strain almost certainly over- estimates the true material strain in the gauge region. The crosshead displacement was recorded as a proxy for the elongation of the gauge length, but no exten- someter was used; in addition, the grips were tightened by hand and some slippage between the specimen and the grips during the test cannot be ruled out. The com- bination of the small gauge length ($L_0$ = 9 mm) and the substantial overall apparatus compliance

IARJSET ISSN (O) 2393-8021, ISSN (P) 2394-1588

International Advanced Research Journal in Science, Engineering and Technology

Impact Factor 8.311 ⁜ Peer-reviewed & Refereed journal ⁜ Vol. 13, Issue 5, May 2026

DOI: 10.17148/IARJSET.2026.13569

amplifies any such artifact: a slippage of only 0.1 mm translates to a spurious strain of $\Delta\varepsilon \approx 0.011$, which is of the order of the elastic strain. The high coefficient of variation of the Young's modulus (32 %) is consistent with this hypothesis.

### 4.2. *Origin of Specimen-to-Specimen Scatter*

Specimen S1 is a clear outlier compared to S2–S4. Two possible explanations can be advanced: (i) a local vari- ation in thickness (the assumed value $t = 0.2$ mm was a nominal one and was not individually measured for each specimen), and (ii) the presence of a critical pre- existing defect close to the gauge region. The micro graphs in Fig. 8–9 show that defects of the order of 15 % of the specimen width are present in the cast film; for a specimen whose true thickness was slightly lower than the nominal value, such a defect would explain both the lower UTS and the lower strain at break observed on S1.

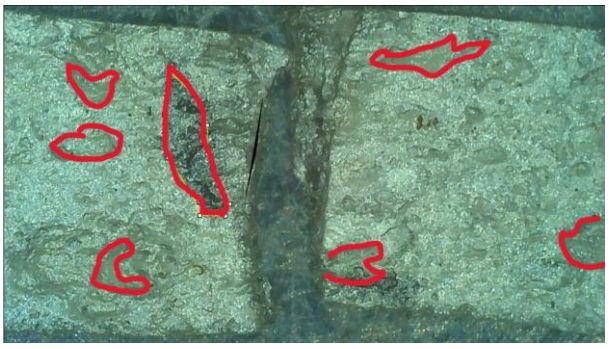

Figure 9: Same micrograph as Fig. 8 with the principal pre-existing porosities outlined in red. The largest defect, located immediately to the left of the fracture path, is approximately 0.4 mm long, comparable to a significant fraction of the specimen width ($w = 3$ mm).

### 4.3. *Limitations of the Study*

The present results should be interpreted with the following limitations in mind:

- The number of specimens (n = 4) is too small for a robust statistical characterization. The standard deviations reported in Table 1 should therefore be considered indicative.
- The loading was applied manually rather than at a constant strain rate. Polysaccharide films are known to be viscoelastic, and the apparent stiff- ness and strength reported here may be lower than what would be measured at a higher strain rate.
- The specimen thickness was not individually verified, and the cross-sectional area was assumed to be uniform along the gauge length. The micro- graphs suggest that this assumption is only ap- proximately valid.
- No control was applied to the ambient relative humidity. Carrageenan and alginate films are strongly hygroscopic, and a higher relative humidity is known to further reduce the stiffness and increase the strain at break [7].

Despite these limitations, the present results provide a baseline characterization of the white *Eucheuma cottonii* / sorbitol / seafood-protein formulation and identify the main parameters (plasticizer mass ratio, residual porosity, drying conditions) that should be the focus of future optimization work. It is also as future work that the seaweed in this work will be mixed with sericin that is obtained from silk cocoon [9, 10]

## 5. CONCLUSION

A bioplastic film was prepared from white *Eucheuma cottonii* seaweed, plasticized with sorbitol and rein- forced with a small fraction of marine protein, and tested in tension on a manual screw-driven apparatus instrumented with an analog force gauge and a digital dial indicator. After removal of the initial take-up artifacts, the four specimens tested exhibited a mean ultimate tensile strength of 2.67(76) MPa, a mean strain at break of $1.0 \pm 0.17$, and a mean Young's modulus of 1.97(62) MPa when determined by linear regression on the initial elastic region. Optical microscopy revealed millimetrescale porosities and an inhomogeneous through-thickness distribution that are identified as the principal mechanical weak points. Com- parison with the literature suggests that the unusually high strain at break and the low stiffness measured here reflect both an over-plasticized formulation and the limitations of the simplified testing setup (no constant strain rate, no extensometer, small gauge length). Future work will focus on: (i) reducing the sorbitol fraction and/or substituting it with a less efficient plasticizer to recover a stiffness closer to the values reported in the literature; (ii) improving the homogeneity of the cast film through vacuum-degassing of the slurry prior to casting; and (iii) repeating the tensile tests on a constant-strain-rate machine equipped with an extensometer, in order to provide values directly comparable to ASTM D638. It is also as future work that the seaweed in this work will be mixed with sericin that is obtained from silk cocoon

DOI: 10.17148/IARJSET.2026.13569

## ACKNOWLEDGEMENTS

I want to thank Udayana University, Bali, Indonesia, for hosting this work during a research internship of the first author from Polytech Lyon, France.

## REFERENCES

[1] ASTM International, *ASTM D638-22, Standard Test Method for Tensile Properties of Plastics*, ASTM International, West Conshohocken, PA, 2022.

[2] A. Saepullah, A. K. Yosua, T. G. T. Nindhia, "*Eu- cheuma cottonii* Seaweed-based Bioplastics: Effects on Raw Material Biochemistry, Extraction Meth- ods, Manufacturing Processes, Mechanical Proper- ties, Applications, and Challenges Faced (A Re- view)," *International Journal Research Publication Analysis*, vol. 2, no. 4, pp. 1–33, April 2026. DOI: 10.1555/ijrpa.8959.

[3] A. Saepullah, A. K. Yosua, T. G. T. Nindhia, "Ef- fect of Temperature Treatment on the Mechan- ical Properties of Bioplastics Edible Film Sea- weed *Gracilaria* Spp.," *International Journal of Re- cent Development in Engineering and Technology (IJRDET)*, vol. 15, no. 4, pp. 1043–1050, April 2026. ISSN: 2347-6435.

[4] K. L. Consebit, K. C. Dermil, E. Y. Magbanua, F.J. Racadio, S. V. Saavedra, H. Abusama, A. Valdez, "Bioplastic from Seaweeds (*Eucheuma Cottonii* ) as an Alternative Plastic," *ASEAN Journal of Science and Engineering*, vol. 2, no. 2, pp. 129–132, 2022.

[5] A. D. Widyanugraha, *Pembuatan dan Karakter- isasi Bioplastik Alginat dari Rumput Laut Sargas- sum Sp.*, Final-year thesis, Jurusan Fisika, Fakultas Matematika dan Ilmu Pengetahuan Alam, Univer- sitas Brawijaya, Malang, Indonesia, 2016.

[6] V. Jost et al., "Influence of plasticisers on the me- chanical and barrier properties of cast biopolymer films," *European Polymer Journal*, 2014.

[7] G. I. Olivas, G. V. Barbosa-Cánovas, "Alginate– calcium films: Water vapor permeability and me- chanical properties as affected by plasticizer and relative humidity," *LWT — Food Science and Tech- nology*, 2008.

[8] "Sargassum-inspired optimized calcium alginate bioplastic composites for food packaging," *Food Hy- drocolloids*, 2022.

[9] A. K. Yosua, A. Saepullah, T. G. T.. Nindhia, Comparative Tensile Strength Analysis of Silk SericinBased Bioplastics with and without Cocoon Powder, International Journal of Recent Development in Engineering and Technology, Volume 15, Issue 4, April 2026), DOI: 10.54380/IJRDET0426_161, PP. 1052-1058

[10] A. K. Yosua, , A. Saepullah, T. G. T. Nindhia, Silk Cocoon As A Biomaterial Platform For Bioplastic Development: A Review, International Journal Research Publication Analysis, Volume: 02 Issue: 04, 27 April 2026, https://doi-doi.org/101555/ijarp.7943, pp. 1-11

 